Response Surface Models Combining Linear and Euler Aerodynamics for HSCT Design

Duane L. Knill*, Anthony A. Giunta†, Chuck A. Baker‡, Bernard Grossman§, William H. Mason¶, Raphael T. Haftka‖, and Layne T. Watson**

Multidisciplinary Analysis and Design Center for Advanced Vehicles

Virginia Polytechnic Institute and State University
Blacksburg, Virginia 24061–0203

Abstract

A method has been developed to efficiently implement supersonic aerodynamic predictions from Euler solutions into a highly constrained, multidisciplinary design optimization of a High-Speed Civil Transport. The method alleviates the large computational burden associated with performing computational fluid dynamics analyses through the use of variable-complexity modeling techniques, response surface methodologies, and coarse grained parallel computing. Using information gained from lower fidelity aerodynamic models, reduced term response surface models representing a correction to the linear theory response surface model predictions are constructed using Euler solutions. Studies into five, ten, fifteen, and twenty variable design problems show that accurate results can be obtained with the reduced term models at a fraction of the cost of creating the full term quadratic response surface models. Specifically, a savings of 255 CPU hours out of 392 CPU hours required to create the full term response surface model is obtained for the twenty variable problem on a single 75 MHz IP21 processor of a SGI *Power Challenge*.

---

*Graduate Research Assistant, Dept. of Aerospace and Ocean Engineering. Current Position: Postdoctoral Research Associate, Dept. of Aeronautics and Astronautics, University of Washington, Seattle, WA, Member AIAA.

†Postdoctoral Research Associate, National Research Council/NASA Langley Research Center, Hampton, VA, Member AIAA.

‡Graduate Research Assistant, Dept. of Aerospace and Ocean Engineering, Student Member AIAA.

§Professor and Dept. Head of Aerospace and Ocean Engineering, Associate Fellow AIAA.

¶Professor of Aerospace and Ocean Engineering, Associate Fellow AIAA.

‖Professor of Aerospace Engineering, Mechanics and Engineering Science, University of Florida, Gainesville, FL, Fellow AIAA

**Professor of Computer Science and Mathematics

1 Introduction

With advances in computational fluid dynamics (CFD) code maturity, grid generation capabilities, and computer performance, the application of CFD in aircraft systems design[1] has received much attention. According to Nicolai,[2] about eighty percent of the aircraft life cycle cost is set at completion of the conceptual design stage. Using more accurate aerodynamic predictions early in the design process, when the aircraft is initially defined, can result in less time and money spent in redesign and an overall improved product. However, the relatively large computational expense associated with CFD analyses can discourage its application in design optimization procedures involving more than a small number of variables. A new method must be developed to enable the efficient implementation of accurate CFD predictions into high dimensional, highly constrained multidisciplinary design optimization (MDO) procedures. This paper presents details and discusses results of such a method as applied to MDO of a High-Speed Civil Transport (HSCT) configuration (Fig. 1).

The main component of this method involves utilizing information gained from inexpensive lower fidelity aerodynamic models to more efficiently create quadratic response surface (RS) models for quantities used to evaluate performance/aerodynamic related constraints. While the specific implementation varies, this approach is based on the ideas of *variable-complexity modeling* (VCM) techniques developed at Virginia Tech.[3–6] In general terms, VCM combines the accuracy of higher fidelity results with the computational efficiency of simpler models.

In this research, simple conceptual level models are used to select an appropriate set of *intervening functions* for which to construct RS models. These RS models are then created using supersonic linear theory aerodynamics. In this paper, 'linear theory aerodynamics' refers to a combination of slender body theory wave drag results, supersonic panel results for the drag due to lift, and a strip boundary layer correction for the viscous drag. Section 3 provides details of these analysis methods. Statistical techniques are applied to the linear theory response surface models to reveal the terms that have a significant impact on calculating the desired aerodynamic quantities. Terms that have little or no effect can be removed without degrading the accuracy of the RS models. Only the important terms are retained when the *reduced term* RS models are constructed using Euler solutions, thereby requiring fewer CFD analyses to compute the coefficients of the models. The reduced term models are created as corrections to the full term linear theory RS models.

Results obtained from the linear theory RS models are also used to identify the likely neighborhood of the optimal designs from Euler analysis. This enables smaller bounds on each design variable, which improves the accuracy of the RS models.

Coarse grained parallel computing comprises the final component of the method, enabling efficient computation of the numerous CFD solutions required. Details of the parallel implementation are presented by Knill *et al.*[7] For consistency, all CPU times presented in this paper are given in terms of single processor performance; however, parallel computation on the 119 node Intel *Paragon* XP/S at Virginia Tech reduced the computational times by factors of over 45 with 53 processors.

Using VCM techniques, RS methodologies, and coarse grained parallel computing has enabled the efficient application of accurate CFD analyses into the combined aerodynamic-structural optimization of a HSCT. This method is tested on HSCT design problems of five, ten, fifteen, and twenty variables.

2 HSCT Design Testbed

The design problem involves minimizing the take-off gross weight (TOGW) of a HSCT with a 5500 $n.mi.$ range, designed to cruise at Mach 2.4 and carry 250 passengers. In this study, the aircraft geometry and mission are parameterized by as many as 20 design variables. Figure 2 shows the aircraft development from the set of design variables. The wing planform is created with eight design variables specifying the root chord, c_{root}; tip chord, c_{tip}; semispan, $b/2$; inboard leading edge (LE) length, s_{LE_I}; inboard LE sweep angle, Λ_{LE_I}; outboard LE sweep angle, Λ_{LE_O}; the inboard trailing edge (TE) length, s_{TE_I}; and the inboard TE sweep angle, Λ_{TE_I}. The airfoil sections are described using five design variables: the leading-edge radius parameter, R_{LE}; location of maximum thickness, $(x/c)_{max\text{-}t}$; and the thickness-to-chord ratios at the wing root, $(t/c)_{root}$, LE break, $(t/c)_{break}$, and wing tip, $(t/c)_{tip}$. The thickness-to-chord ratio is varied linearly between these three spanwise locations. The fuselage radii, r_{fus_i}, are specified at four axial *restraint* locations. The shape of the body between these points is then determined by considering it as a minimum wave drag body of a fixed volume.[3,8] The final variables specify the inboard nacelle placement, y_{nac}, the separation between the inboard and outboard nacelles, Δy_{nac}, and fuel weight, W_{fuel}. The allowable ranges of values for these variables are shown in Table 1. The vertical tail shape, engine thrust, relative position of the wing to the fuselage, and the cruise climb rate and altitude are fixed.

The optimization uses up to 50 inequality constraints dealing with the aircraft geometry and performance/aerodynamics. These constraints (Table 2) are devised to ensure feasible aircraft geometries and impose realistic performance and control capabilities. Fuel volume and wing chord length limits are examples of geometric constraints. Performance/aerodynamic constraints include, for example, landing angle-of-attack limits and wing, tail, and engine scrape prevention criteria. Emergency conditions are used to enforce the landing constraints. It is assumed that the aircraft lands on a runway 5000 ft above sea level at 145 $knots$, carrying 50% of its initial fuel weight. These are complicated, nonlinear constraints that require aerodynamic forces and moments, stability and control derivatives, and center of gravity and inertia estimates.

An example of the complicated constraint boundaries present in the design spaces associated with this HSCT optimization is shown in Fig. 3. This figure represents a plane in ten dimensional design space, passing through three design points. Two of the design points represent local optima found by the optimizer, and the third point is a suboptimal feasible point. The design points represented by the open circles are feasible points, while those represented by the filled circles have violated some constraints. The plot illustrates the nonconvexity of the design space caused by the aerodynamic constraints. If the optimizer drives the design near Optimum 1, it cannot cross the boundary created by the range constraint to arrive at Optimum 2 which is 2000 *lb* lighter. In addition to enabling the rapid creation of these types of useful plots, using RS modeling techniques allows one to investigate a number of different starting points in the optimization to discover these local optima. The bulk of the computational effort is spent initially on the creation of the RS models, and performing a number of optimizations using the polynomial RS models is relatively inexpensive.

A series of optimization problems of five, ten, fifteen, and twenty variables serve to evaluate our methods of including Euler analyses in multidisciplinary HSCT design. The design variables (Table 1) and constraints (Table 2) for the simplified problems are subsets of those used in the twenty variable design. The upper and lower limits of the active design variables remain the same throughout the series of optimization problems. These bounds on the design variables are selected from optimization results performed using the linear theory RS models. For the five, ten, and fifteen variable problems we can afford the evaluations required to create full term quadratic RS models, providing us with a means to assess the performance of the reduced term models.

3 HSCT Design Tools

3.1 Linear Theory Aerodynamics

What we term supersonic linear theory predictions are actually obtained from three codes, each computing a particular component of the drag. The volumetric wave drag is computed using the Harris[9] wave drag program. Drag due to lift is calculated using a panel method by Carlson *et al.*[10] with attainable leading edge thrust corrections.[11] Viscous drag estimates are obtained using standard algebraic estimates[12] of the skin friction assuming turbulent flow. These viscous drag predictions are also added to the Euler solutions.

Wing camber for the HSCT designs is determined using a linear theory code with empirical corrections to account for nonlinear effects named WINGDES.[10,13] WINGDES attempts to find the camber distribution along the wing which minimizes the drag due to lift. Two runs of WINGDES per design were required to get the proper camber distribution. The second run serves to smooth the camber distribution and provide the maximum leading edge suction parameter at the design lift coefficient.

3.2 Computational Fluid Dynamics

Version 2.2 of the General Aerodynamic Simulation Program[14] (GASP) is used to obtain the Euler solutions. GASP is a fully conservative CFD code which solves the Reynolds averaged Navier-Stokes equations and many of its subsets. The code uses an upwind three dimensional finite volume spatial discretization and, for our calculations, a third order upwind biased interpolation of the Roe fluxes is used in each of the marching planes. Space marching has been performed for all of the CFD calculations. The accuracy of the CFD predictions has been studied extensively by Knill *et al.*[15] These studies confirmed that the Euler drag results are accurate within 1/2 count[††] in the range of flight conditions considered using 405,000 grid cells.

Grids suitable for space marching calculations on the HSCT wing-fuselage configurations are created using a grid generator originally developed by Barger.[16] The code was modified[17] to provide better resolution of the leading edge and remain robust for large changes in the aircraft geometry. The grid generator receives as input the aircraft configuration stored in the Craidon[18] geometry format, extends the wing to join the fuselage, performs filleting of the wing-fuselage intersection, and then creates a grid for space marching calculations. Two marching planes for a wing-fuselage configuration are shown in Fig. 4. Since our HSCT optimization code creates a Craidon description file from its set of design variables, the conversion from a set of design variables to a space marching CFD grid is straightforward. The grid generator is automated and robust for large planform changes, essential qualities for application in design optimization.

3.3 Weight Estimation

All components of the TOGW are calculated using empirically based functions obtained from the Flight Optimization System[19] (FLOPS) weight equations.

3.4 Optimization Routine

Optimization is performed using the software package Design Optimization Tools[20] (DOT). The constrained optimization is performed using sequential quadratic programming and central difference gradient approximations. The optimization problem is the minimization of the TOGW subject to a number of constraints related to both the geometry and the mission. Side constraints limit the values of the design variables. The optimization problem can be written as

$$\begin{aligned} &\min_{\mathbf{x}\in\Re^m} TOGW(\mathbf{x}), \qquad (1)\\ &\text{subject to:} \quad \mathbf{g}(\mathbf{x}) \leq 0,\\ &\qquad\qquad\quad \mathbf{x_{min}} \leq \mathbf{x} \leq \mathbf{x_{max}} \end{aligned}$$

[††] $\Delta C_D = 1.0\times10^{-4}$ corresponds to 1 count of drag

where $\mathbf{x}$ is the m-dimensional vector of design variables, and $\mathbf{g}(\mathbf{x})$ is the vector of nonlinear inequality constraints. The minimum and maximum values of the design variables are given by $\mathbf{x_{min}}$ and $\mathbf{x_{max}}$.

4 Response Surface Modeling

To use relatively expensive Euler solutions for the large number of constraint evaluations required in our multidisciplinary optimization, RS models of the supersonic aerodynamics are created. Response surface modeling techniques for aerodynamic and structural design improve the performance of highly constrained gradient based optimizations.[6, 21–23] The RS models smooth out numerical noise present in the analyses. Numerical noise manifests itself as low amplitude, high frequency variations in the computational results with changes in the design variables. These variations are present in any method with iterative procedures or discrete representations of continuous geometric shapes or physical phenomena. This noise distorts gradient information and can lead to artificial local minima in the design space. In addition, the analysis codes are separated from the optimization routines, eliminating the need to integrate large, production level grid generators, analysis codes, and post processing utilities with the optimizer. This also allows analyses to be performed by experts in the specific discipline on parallel architecture machines. Finally, by replacing complex analysis codes with simple quadratic polynomials, one can readily obtain information on design trade-offs, sensitivities to certain variables, and insight into the highly constrained, nonconvex design spaces. Details of these aspects are presented by Knill *et al.*[7]

4.1 Functional Form of the Response

Not all response functions can be modeled accurately by low order polynomials, but often accuracy can be improved by transformations of the function or its arguments. Analytic solutions obtained under simplifying assumptions often help reveal the needed transformations. The use of such transformations was pioneered for approximations of structural response by Schmit and Vanderplaats and their coworkers (see Ref. 24). They called the transformed variables and functions 'intervening variables' and 'intervening functions,' respectively.

Our group has made use of intervening variables to improve the accuracy of the RS model for optimal structural weight as a function of the HSCT configuration variables.[5] Golovidov[25] showed that approximating the drag coefficient by a quadratic polynomial and calculating the range from the drag coefficient improves the accuracy over direct approximation of the range. The drag coefficient became the intervening function for the range.

In the present work, we use the knowledge that for uncambered wings the drag coefficient is approximately a simple quadratic function of the lift coefficient, written as

$$C_D(\mathbf{x}) = C_{D_0}(\mathbf{x}) + K(\mathbf{x})\ {C_L}^2. \tag{2}$$

We then fit the intervening functions, $C_{D_0}(\mathbf{x})$ and $K(\mathbf{x})$, by quadratic RS models. Using this form has the added advantage of removing the dependence of the drag coefficient on the fuel weight, introduced only through the lift coefficient.

The HSCT wings have little camber since they are optimized for cruise at Mach 2.4; therefore, this form of the drag polar for uncambered wings is still fairly accurate. The error in fitting the Euler drag polars to this form is less than 0.5 count over $0.05 \leq C_L \leq 0.12$. These values of C_L cover the range of cruise lift coefficients found for our HSCT designs.

4.2 Creating Quadratic RS Models

A quadratic response surface model in m variables has the form

$$y = c_0 + \sum_{1 \leq j \leq m} c_j\, x_j + \sum_{1 \leq j \leq k \leq m} c_{jk}\, x_j\, x_k, \tag{3}$$

where y is the response, the x_j are the design variables, and c_0, c_j, and c_{jk} are the polynomial coefficients. There are $(m+1)(m+2)/2$ coefficients for a quadratic response surface model in m variables. Using approximately twice as many points as the number of coefficients is sufficient to accurately compute the value of the coefficients for problems with five variables. However, as the dimension of the problem increases, the ratio of the required number of points to the number of terms p/n in the response surface also increases. We use a systematic increase from $p/n = 2.0$ in the five variable case to $p/n = 3.5$ in the twenty variable case to provide adequate accuracy. This translates to 60, 276, 720, and 1470 CFD evaluations per RS model for the 5, 10, 15, and 20 variable problems, respectively.

To compute the coefficients for the quadratic RS models of both $C_{D_0}(\mathbf{x})$ and $K(\mathbf{x})$ for a 30 variable problem would require 4184 CFD evaluations. On a single processor of the SGI *Power Challenge*, this would require over 46 days of computation! Clearly, a method must be developed which enables accurate response surface estimates with a reduced number of required CFD analyses.

4.3 Point Selection

Design of experiments theory provides a systematic means of selecting the set of points (called an *experimental design*) within the m-dimensional design space. The number of points in this initial screening experimental design is reduced by applying geometric constraints. Using the remaining set of geometrically feasible points, the D-optimality criterion[26] is applied to select the points used in creating the RS models. Knill *et al.*[7] provide further details on the experimental design and RS model creation.

4.4 Reduced Term RS Models

Linear theory RS models can be readily created for moderately high dimensional spaces because the evaluations are computationally inexpensive. *Stepwise regression analysis* provides a means of systematically removing terms from the RS models that have little or no impact on the response. Terms are eliminated using a measure of the significance level of the term called the p-value. This represents the probability that the coefficient of a particular term is actually zero, not the value computed. Typically, a p-value of 0.05 or less indicates that the term is significant in predicting the variation in the response. As the prescribed value of the p-value is reduced, more terms are eliminated from the RS model. At some point in the stepwise regression process, the error in the RS model fit increases noticeably, indicating that too many terms have been eliminated to satisfy the p-value limit. For this research, JMP[27] is used to perform the stepwise regression analysis.

The stepwise regression technique is applied to the RS models for the linear theory aerodynamics to create *reduced term* RS models. Since the Mach 2.4 cruise regime is predominantly linear, performing stepwise regression analysis on the RS models for the linear theory aerodynamics should give polynomials with the terms that are also important with respect to Euler aerodynamics. Instead of creating full term quadratic RS models for the Euler results, one needs only to create the reduced term models found using linear theory analyses. Computational time is therefore not wasted evaluating coefficients which do not have a significant effect on the response.

The root mean square (RMS) error estimate is used to indicate the error in the RS model fit. The RMS error is calculated as

$$\text{RMS error} = \sqrt{\frac{\sum_{i=1}^{N} (y_i - \hat{y}_i)^2}{N}}, \tag{4}$$

where y_i is the observed value of the response and $\hat{y}_i$ is the predicted value of the response at the N sample points. The N sample points are a randomly selected subset of the points used in the initial screening experimental design, not including the design points used in the RS model creation.

4.5 Incremental RS Models

We have found that the best means to implement the reduced term RS models with Euler analyses is by using an *incremental* form. (See Ref. 17 for details on other alternatives.) This approach uses reduced term RS models for the difference between the Euler and linear theory RS model predictions, $\Delta C_{D_0}(\mathbf{x})$ and $\Delta K(\mathbf{x})$. To estimate the Euler values of the response, these *correction* RS models are added to the full term quadratic linear theory RS models. The sum of the linear theory and correction RS models will be referred to as the incremental

RS models (*i.e.*, n term incremental RS model = n term correction RS model + full term linear theory RS model).

5 Optimization Results

Results from stepwise regression analysis for the five variable design are shown in Fig. 5. The RMS error in the linear theory RS models represents the differences between the linear theory RS model prediction of the cruise drag and the linear theory analysis value. The RMS error in the incremental RS models represents the differences between the incremental RS model prediction of the cruise drag and the actual Euler value. Both errors are computed at 30 points randomly selected from the set of feasible design points not used in the RS model creation. The plot shows that the RMS error for the incremental RS models does not have the abrupt increase below seven terms that is present in the linear theory RS models.

The stepwise regression plot demonstrates that the stepwise regression technique can eliminate unimportant terms from the response surface models with little or no effect on the error. Furthermore, it shows that the errors in the reduced term incremental RS models, created using terms found from stepwise regression analysis on the linear theory RS models, do not change significantly as the number of terms is reduced. This indicates that linear theory analysis does reveal the terms that are important to the Euler analyses. The five term incremental RS models, which require only 10 design points to be evaluated, are chosen to perform the five variable optimization studies.

The five term incremental RS model requires only 5.3 hours to create, compared to 16 hours required for the full term model. The optimal design obtained from the incremental RS models compares well (Fig. 6) to the full term Euler RS model. The left half of this figure contains the optimal designs for the five variable problem. More importantly, Euler analysis on the optimal design reveals that the RS model cruise drag prediction is less than 0.1 count higher than the Euler value. The design variable values (Table 3) for the incremental RS model optimum fall within their prescribed bounds, demonstrating the success of selecting these bounds based on the linear theory optimal designs. Table 4 shows that the corrected TOGW (W_{C-TOGW}) of $622,500\,lb$ is only $700\,lb$ higher than that for the full term Euler optimum. The corrected TOGW is the result of adding or subtracting fuel weight (ΔW_{fuel}) to the optimal designs in order to correct for the range discrepancy caused by differences between the RS model and actual Euler predictions.

For the ten and fifteen variable designs, using the reduced term incremental RS models results in savings of 47 out of 74 hours and 115 out of 192 hours required to create the full term RS models, respectively. The error in RS model drag prediction for both cases is within 0.6 counts of the value from Euler analysis. Details of these cases are presented by Knill *et al.*[7]

Due to computational expense, the full quadratic Euler RS models are not created for the twenty variable design. This is exactly the situation for which the reduced term incremental RS models were developed. Regression analysis on the linear theory data (Fig. 7) shows that the RMS cruise drag error remains nearly constant until about 73 of the original 210 terms remain in the RS models. Creating the 73 term RS models requires data from 256 of the 735 total experimental design points. Euler evaluations for 350 design points were performed to create the 100 term incremental RS models. Since the full term Euler RS models are not present, this provides a model with which to compare the errors in the 73 term RS models. It is seen that there is no major difference in the cruise drag errors of the 100 term and 73 term incremental RS models.

The optimal design from the incremental RS models is shown in Fig. 6 to provide comparison with the five variable optima. Table 3 provides the optimal design variable values. The cruise drag prediction for the optimal design from the incremental RS models is 0.8 counts lower than the actual Euler value, which is much better than the RMS error estimate of the RS models. Compensating for the range deficiency gives a corrected TOGW of $588,000\,lb$. Table 4 shows the consistent reduction in the optimal wing weight, fuel weight, and TOGW with increasing number of design variables.

Using the reduced term incremental RS models has provided a means to create RS models for high dimensional problems where computing the coefficients of the full quadratic RS models is not viable. Figure 8 shows how the present method extrapolates to 25 and 30 design variables. The trend indicates that a reduced term response surface model in 25 design variables can be created using the same number of terms as a full quadratic model in 15 design variables.

5.1 RS Model Accuracy

The RMS error estimates for the incremental RS models are consistently higher than the errors in the optimal designs. Investigation led to the finding that the incremental RS model fit through the interior of the design bounding box is better than that at the vertices, where the points used to evaluate the RMS errors are located. When evaluating the RMS error in the fifteen variable design using a new set of 162 design points scattered through the interior of the design box, the RMS error estimate dropped from 1.5 counts to 0.9 count. This indicates that using points selected only from the vertices of the design box may not provide a sufficiently accurate representation of the RS model fit.

The RMS errors in the linear theory and incremental RS models steadily increase from the 5 variable through the 20 variable problem. Preliminary examinations of three methods to improve the accuracy of the RS models have been made. The first method involves using a more accurate physical model to provide the functional form for the drag polar. With an additional CFD evaluation per design, a more accurate cambered form of the drag polar,

$C_D(\mathbf{x}) = C_{D_m}(\mathbf{x}) + K(\mathbf{x})\ \ [C_L - C_{L_m}(\mathbf{x})]^2$, can be evaluated. This approach was found to reduce the RMS error in the RS models by approximately 0.3 drag count. The nonquadratic nature of the response can be addressed in two ways: reducing the size of the design bounding box and including cubic terms in the RS model. Reducing the size of the design box has a significant effect on the error; however, care must be taken to ensure that the optimal design lies within the reduced box. Including cubic terms allows one to maintain the size of the original box, but the computational expense of evaluating all the cubic terms makes it unattractive for high dimensional problems. Using the more accurate drag polar along with a "zooming" technique to reduce the size of the design box appears to be a promising approach.

6 Conclusions

A method for efficiently implementing supersonic Euler analyses in a combined aerodynamic-structural optimization of a High-Speed Civil Transport configuration has been developed and tested on problems of five, ten, fifteen, and twenty design variables. This method takes advantage of information obtained from inexpensive lower fidelity aerodynamic analyses to more effectively create response surface models for the Euler solutions. The functional form of the drag polar is selected based on conceptual level aerodynamic models. *Correction* response surface models representing the difference between linear theory and Euler values of the intervening functions, $\Delta C_{D_0}(\mathbf{x})$ and $\Delta K(\mathbf{x})$, are then created. *Incremental* response surface models for the Euler predictions are then created by adding the correction response surface models to the full quadratic linear theory response surface models. Optimization results from the linear theory response surface models are used to select the design bounding box within which the optimum from Euler analysis should lie. This improves the accuracy of the response surface models by allowing smaller ranges on the design variables compared to those required if no information was available on the general location of the optimal design.

Computational expense is reduced using stepwise regression analysis results gained from linear theory analysis to remove terms from the response surface models that are not important to the Euler aerodynamics. Compared to the cost of creating full term response surface models, creating the reduced term response surface models results in savings of 11 out of 16 hours, 47 out of 74 hours, 115 out of 192 hours, and 255 out of 392 hours of CPU time on a single 75 MHz IP21 processor of a SGI *Power Challenge* for the five, ten, fifteen, and twenty variable design problems, respectively. Errors in the incremental response surface model cruise drag predictions, based on actual Euler calculations, for the optimal designs range from 0.1 counts to 0.8 counts.

Acknowledgments

Support for this research was provided through the NASA Langley Research Center grants NAG1–1160 with Mr. Peter Coen as contract monitor and NAG1–1562 with Dr. Perry Newman as contract monitor.

References

1. J. P. Geising, S. Agrawal, and B. K. Bharadvaj. "The Role of Computational Fluid Dynamics in Multidisciplinary Design Optimization of Transport Aircraft," *Proceedings of the Sixth International Symposium on Computational Fluid Dynamics, Technology, and Operations Congress*, Lake Tahoe, CA, September 4–7, 1995.

2. L. M. Nicolai. *Fundamentals of Aircraft Design*, E.P. Domicone Printing Services, Fairborne, OH, pp. 24-23–24-25, 1975.

3. M. G. Hutchison, E. R. Unger, W. H. Mason, B. Grossman, and R. T. Haftka. "Variable-Complexity Aerodynamic Optimization of a High-Speed Civil Transport Wing," *Journal of Aircraft*, 31, No. 1: 110–116, 1994.

4. A. A. Giunta, R. Narducci, S. Burgee, B. Grossman, W. H. Mason, L. T. Watson, and R. T. Haftka. "Variable-Complexity Response Surface Aerodynamic Design of an HSCT Wing," AIAA Paper No. 95–1886, 1995.

5. M. Kaufman, V. Balabanov, S. L. Burgee, A. A. Giunta, B. Grossman, W. H. Mason, L. T. Watson, and R. T. Haftka. "Variable-Complexity Response Surface Approximations for Wing Structural Weight in HSCT Design," AIAA Paper No. 96–0089, 1996.

6. V. Balabanov, M. Kaufman, D. L. Knill, D. Haim, O. Golovidov, A. A. Giunta, R. T. Haftka, B. Grossman, W. H. Mason, and L. T. Watson. "Dependence of Optimal Structural Weight on Aerodynamic Shape for a High-Speed Civil Transport," AIAA Paper No. 96–4046, 1996.

7. D. L. Knill, A. A. Giunta, C. A. Baker, B. Grossman, W. H. Mason, R. T. Haftka, and L. T. Watson. "Multidisciplinary HSCT Design using Response Surface Approximations of Supersonic Euler Aerodynamics," AIAA Paper No. 98-0905, 1998.

8. E. Eminton. "On the Minimization and Numerical Evaluation of Wave Drag," *Royal Aircraft Establishment Report AERO.2564*, November 1955.

9. R. V. Harris, Jr. "An Analysis and Correlation of Aircraft Wave Drag," NASA TM X–947, 1964.

10. H. W. Carlson and D. S. Miller. "Numerical Methods for the Design and Analysis of Wings at Supersonic Speeds," NASA TN D–7713, 1974.

11. H. W. Carlson and R. J. Mack. "Estimation of Leading-Edge Thrust for Supersonic Wings of Arbitrary Planforms," NASA TP–1270, 1978.

12. E. J. Hopkins. "Charts for Predicting Turbulent Skin Friction from the van Driest Method (II)," NASA TN D–6945, October 1972.

13. H. W. Carlson and K. B. Walkley. "Numerical Methods and a Computer Program for Subsonic and Supersonic Aerodynamic Design and Analysis of Wings with Attainable Thrust Corrections," NASA CR–3808, 1984.

14. W. D. McGrory, D. C. Slack, M. P. Applebaum, and R. W. Walters. *GASP Version 2.2 Users Manual*, Aerosoft, Inc., Blacksburg, VA, 1993.

15. D. L. Knill, V. Balabanov, O. Golovidov, B. Grossman, W. H. Mason, R. T. Haftka, and L. T. Watson. "Accuracy of Aerodynamic Predictions and Its Effects on Supersonic Transport Design," *MAD Center Report 96–12–01*, Multidisciplinary Analysis and Design Center for Advanced Vehicles, Virginia Tech, Blacksburg, VA, December 1996.

16. R. L. Barger, M. S. Adams, and R. R. Krishnan. "Automatic Computation of Euler-Marching and Subsonic Grids for Wing-Fuselage Configurations," NASA TM 4573, July 1994.

17. D. L. Knill. *Implementing Aerodynamic Predictions from Computational Fluid Dynamics in Multidisciplinary Design Optimization of a High-Speed Civil Transport*, Ph.D. thesis, Department of Aerospace and Ocean Engineering, Virginia Polytechnic Institute and State University, also found in MAD Center Report 97–12–01, 1997.

18. C. B. Craidon. "Description of a Digital Computer Program for Airplane Configuration Plots," NASA TM X–2074, 1970.

19. L. A. McCullers. "Aircraft Configuration Optimization Including Optimized Flight Profiles," *Proceedings of Symposium on Recent Experiences in Multidisciplineary Analysis and Optimization,* J. Sobieski, compiler, NASA CP–2327, pp. 396–412, April 1984.

20. Vanderplaats Research & Development, Inc. *DOT Users Manual, Version 4.20*, Colorado Springs, CO, 1995.

21. A. A. Giunta, V. Balabanov, D. Haim, B. Grossman, W. H. Mason, L. T. Watson, and R. T. Haftka. "Multidisciplinary Optimisation of a Supersonic Transport Using Design

of Experiments Theory and Response Surface Modelling," *The Aeronautical Journal of the Royal Aeronautical Society*, 101, No. 1008: 347–356, October 1997.

22. R. S. Sellar, M. A. Stelmack, S. M. Batill, and J. E. Renaud. "Response Surface Approximations for Discipline Coordination in Multidisciplinary Design Optimization," AIAA Paper No. 96–1383, 1996.

23. W. Chen, J. K. Allen, D. P. Schrage, and F. Mistree. "Statistical Experimentation Methods for Achieving Affordable Concurrent Systems Design," *AIAA Journal*, 35, No. 5, May 1997.

24. R. T. Haftka and Z. Gürdal. *Elements of Structural Optimization*, Kluwer, 3rd edn., pp. 211–219, 1992.

25. O. Golovidov. "Variable-Complexity Response Surface Approximations for Aerodynamic Parameters in HSCT Optimization," *MAD Center Report 97–06–01*, Multidisciplinary Analysis and Design Center for Advanced Vehicles, Virginia Tech, Blacksburg, VA, June 1997.

26. M. J. Box and N. R. Draper. "Factorial Designs, the $\mid \mathbf{X}^T\mathbf{X} \mid$ Criterion, and Some Related Matters," *Technometrics*, 13, No. 4, pp. 731–742, 1971.

27. SAS Institute, Inc. *JMP Users Guide, Version 3.1*, Cary, NC, 1995.

Table 1: Design Variable Limits in the Optimization Problems.

Variable	# of Variables			
	5	**10**	**15**	**20**
Planform Variables				
c_{root}	$150 - 190\,ft$			
c_{tip}	$7 - 13\,ft$			
$b/2$	$[74\,ft]$	$58 - 78\,ft$		
s_{LE_I}	$[132\,ft]$		$105 - 135\,ft$	
Λ_{LE_I}	$67° - 76°$			
Λ_{LE_O}	$[25°]$	$12° - 32°$		
s_{TE_I}	straight TE			$10 - 30\,ft$
Λ_{TE_I}	straight TE			-55° − 16°
Airfoil Variables				
$(x/c)_{max\text{-}t}$	[40%]	$38 - 52\%$		
R_{LE}	[2.5]	$2.1 - 4.1$		
$(t/c)_{root}$	$1.5 - 2.7\%$			
$(t/c)_{break}$	$(t/c)_{break} = (t/c)_{root}$			$1.5 - 2.7\%$
$(t/c)_{tip}$	$(t/c)_{tip} = (t/c)_{root}$			$1.5 - 2.7\%$
Fuselage Variables				
r_{fus_1}	$[5.2\,ft]$		$4.5 - 6.0\,ft$	
r_{fus_2}	$[5.7\,ft]$		$4.5 - 6.0\,ft$	
r_{fus_3}	$[5.9\,ft]$		$4.5 - 6.0\,ft$	
r_{fus_4}	$[5.5\,ft]$		$4.5 - 6.0\,ft$	
Nacelle and Mission Variables				
y_{nac}	$[20\,ft]$	$10 - 35\,ft$		
Δy_{nac}	$[6\,ft]$			$6 - 18\,ft$
W_{fuel}	No Limits			

$[\cdot]$ variable value when not active in the design

Table 2: Constraints Applied in the Optimization Problems.

#	Constraint	# of Variables 5	10	15	20
1	Range $\geq 5,500\, n.mi.$	X	X	X	X
2	C_L at landing speed	X	X	X	X
3–20	Section $C_\ell \leq 2$	X	X	X	X
21	Landing $\alpha \leq 12°$		X	X	X
22	Fuel volume	X	X	X	X
23	Spike prevention	X	X	X	X
24–41	Wing chord $\geq 7.0\, ft$	X	X	X	X
42–43	Engine scrape		X	X	X
44–45	Engine scrape (5° roll)		X	X	X
46	Wing tip scrape		X	X	X
47	TE break scrape (5° roll)		X	X	X
48	LE break $\leq$ semispan	X	X	X	X
49	TE break $\leq$ semispan				X
50	Engine-out limit; (vertical tail design)	X	X	X	X
	# of Applied Constraints	**42**	**49**	**49**	**50**

Table 3: Design Variable Values for the Optimal Designs from Incremental RS Models.

Variable	**# of Variables**			
	5	**10**	**15**	**20**
Planform Variables				
c_{root} (ft)	178.0	170.4	166.2	169.5
c_{tip} (ft)	7.4	9.0	7.7	7.8
$b/2$ (ft)	[74.0]	72.1	68.1	67.4
s_{LE_I} (ft)	[132.0]		120.4	124.8
Λ_{LE_I} (deg)	71.1	70.0	69.4	70.5
Λ_{LE_O} (deg)	[25.0]	18.7	24.2	30.4
s_{TE_I} (ft)	straight TE			27.4
Λ_{TE_I} (deg)	straight TE			-29.0
Airfoil Variables				
$(x/c)_{max\text{-}t}$	[40.0%]	50.2%	49.8%	51.1%
R_{LE}	[2.5]	2.1	2.1	2.1
$(t/c)_{root}$	1.81%	1.91%	1.99%	1.99%
$(t/c)_{break}$	$(t/c)_{break} = (t/c)_{root}$			1.91%
$(t/c)_{tip}$	$(t/c)_{tip} = (t/c)_{root}$			1.94%
Fuselage Variables				
r_{fus_1} (ft)	[5.2]		5.2	5.2
r_{fus_2} (ft)	[5.7]		5.6	5.6
r_{fus_3} (ft)	[5.9]		5.6	5.6
r_{fus_4} (ft)	[5.5]		5.2	5.2
Nacelle and Mission Variables				
y_{nac} (ft)	[20.0]	30.0	28.1	27.7
Δy_{nac} (ft)	[6.0]			6.0
W_{fuel} (lb)	309,800	306,000	299,600	293,300

$[\cdot]$ variable value when not active in the design

Table 4: Weights for Optimal Designs from Full Term and Reduced Term RS Models.

	# of Variables			
	5	**10**	**15**	**20**
Reduced Term Incremental RS Models				
W_{wing}	$103,900$	$96,100$	$87,800$	$86,900$
W_{fuel}	$309,800$	$306,000$	$299,600$	$293,300$
W_{TOGW}	$622,800$	$610,400$	$590,700$	$583,200$
Range:				
(Euler)	5503	5542	5495	5449
ΔW_{fuel}	-320	-3720	450	4430
W_{C-TOGW}	$622,500$	$606,300$	$591,200$	$588,000$
Full Term Euler RS Models				
W_{wing}	$103,900$	$99,200$	$87,900$	
W_{fuel}	$313,200$	$301,000$	$300,100$	
W_{TOGW}	$626,300$	$608,900$	$591,500$	
Range:				(N/A)
(Euler)	5544	5485	5505	
ΔW_{fuel}	-4010	1300	-440	
W_{C-TOGW}	$621,800$	$610,300$	$591,000$	

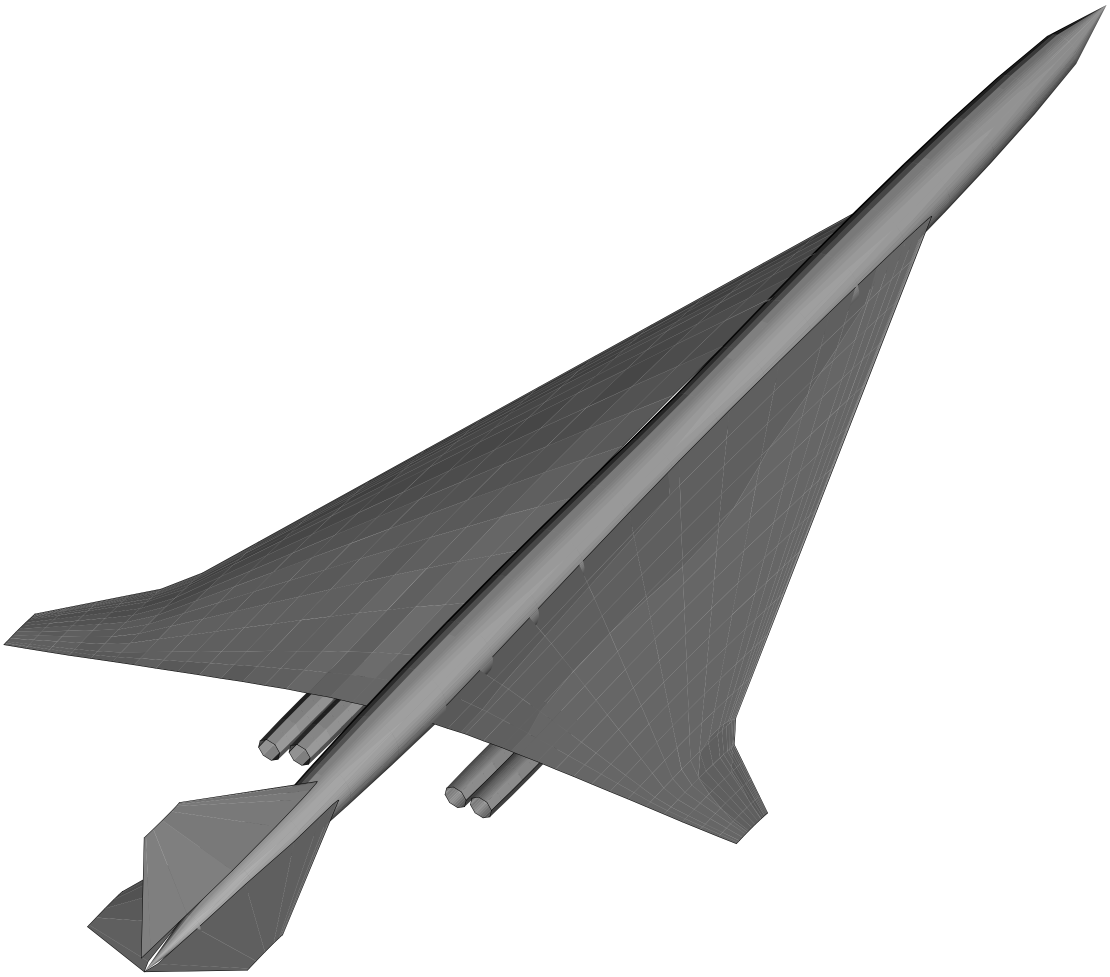

Figure 1: Typical HSCT Configuration.

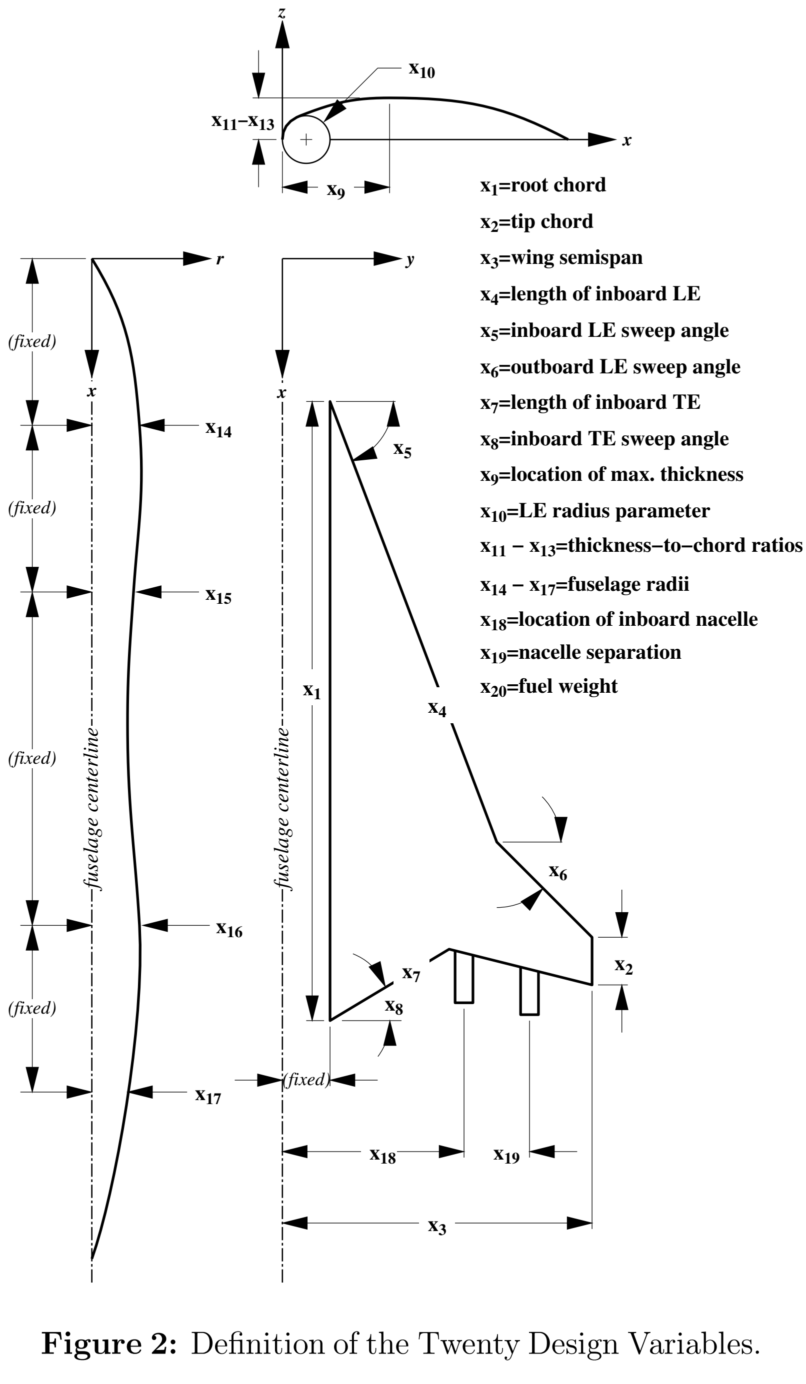

Figure 2: Definition of the Twenty Design Variables.

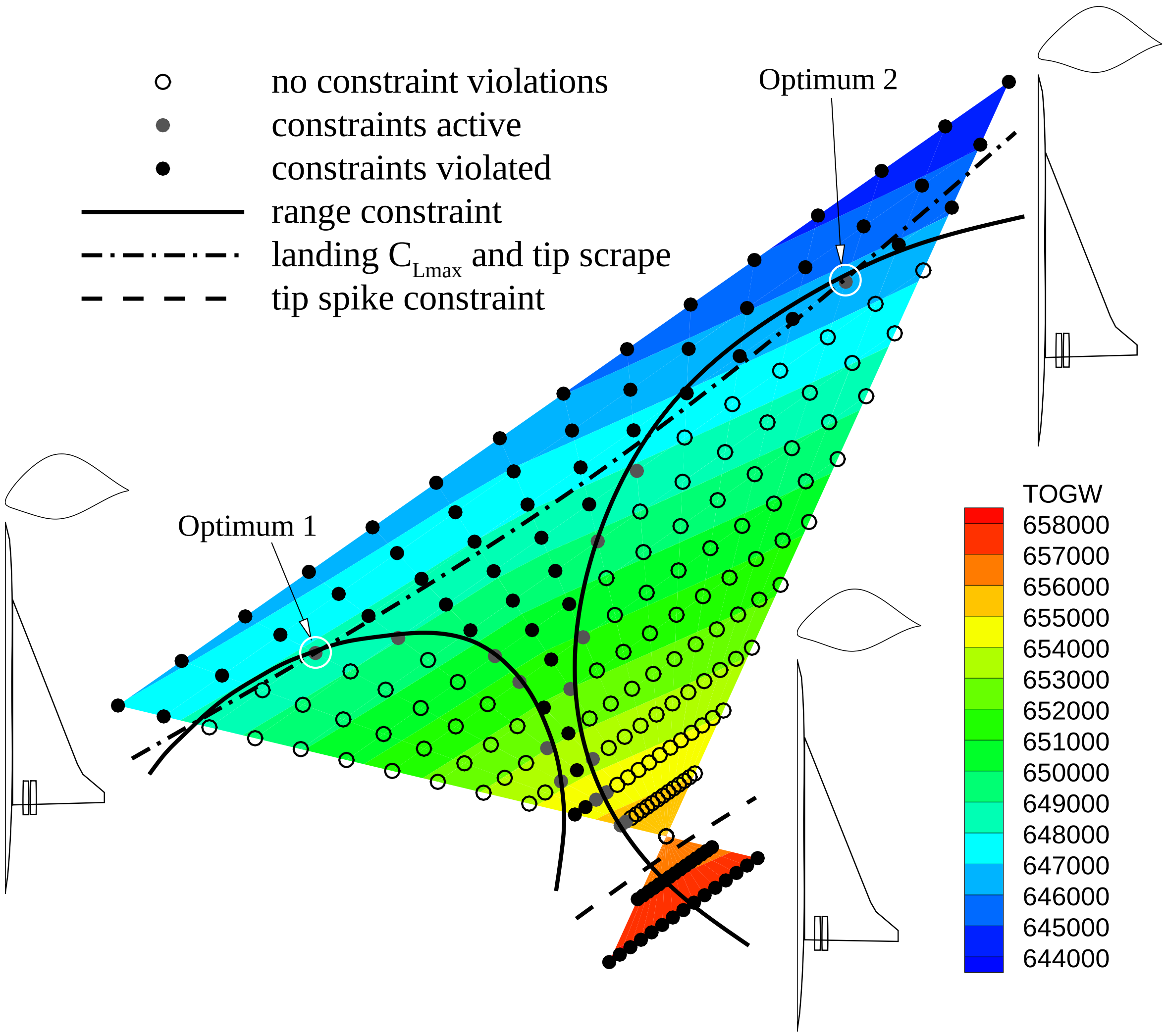

Figure 3: Nonconvex Design Space in a Ten Variable Problem.

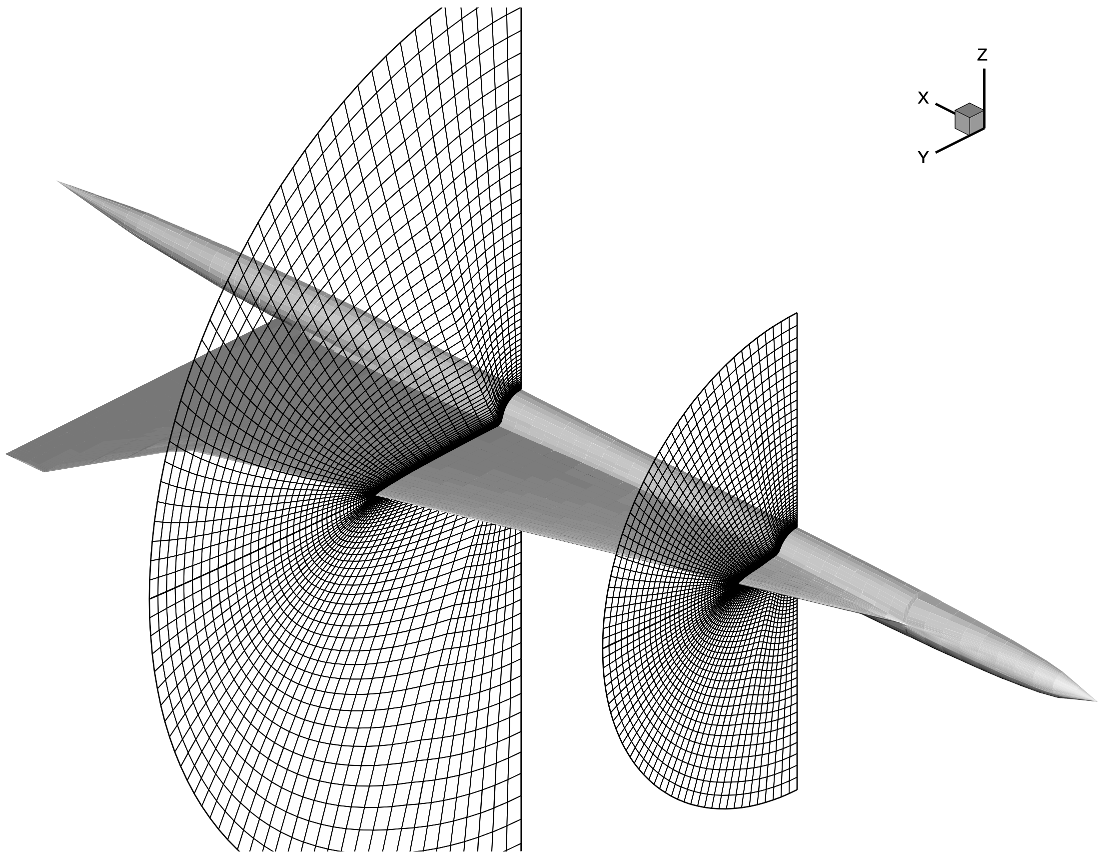

Figure 4: HSCT with CFD Grid Planes.

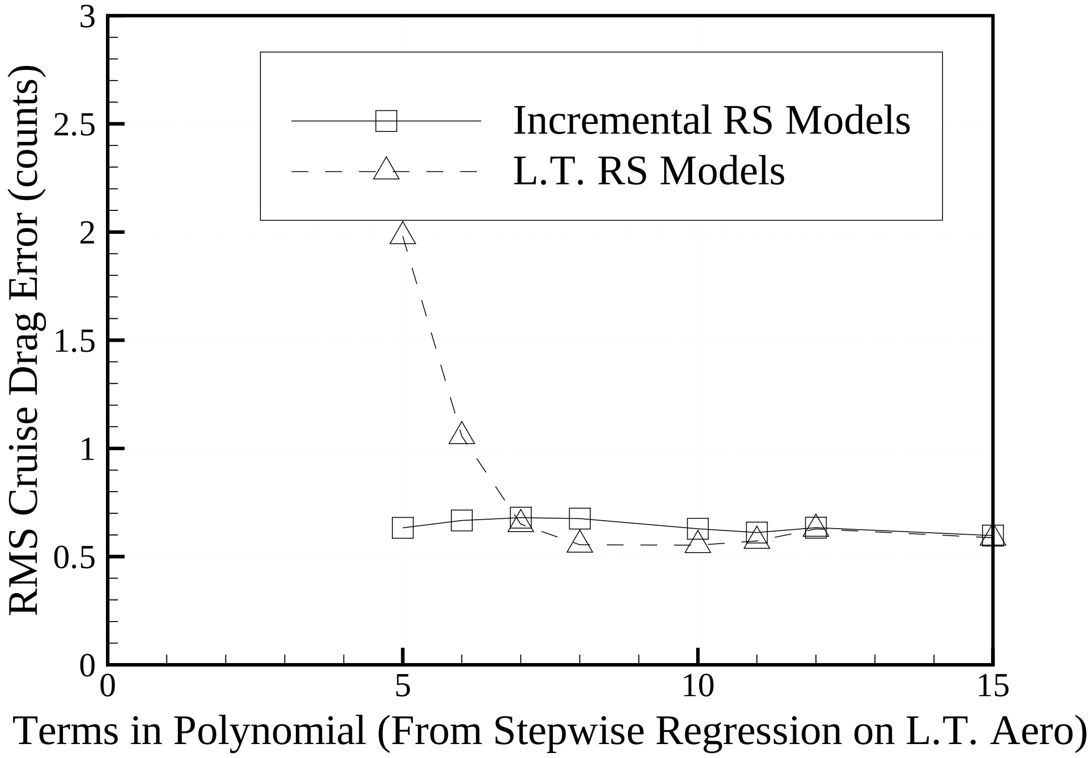

Figure 5: Stepwise Regression (5 Variable Problem).

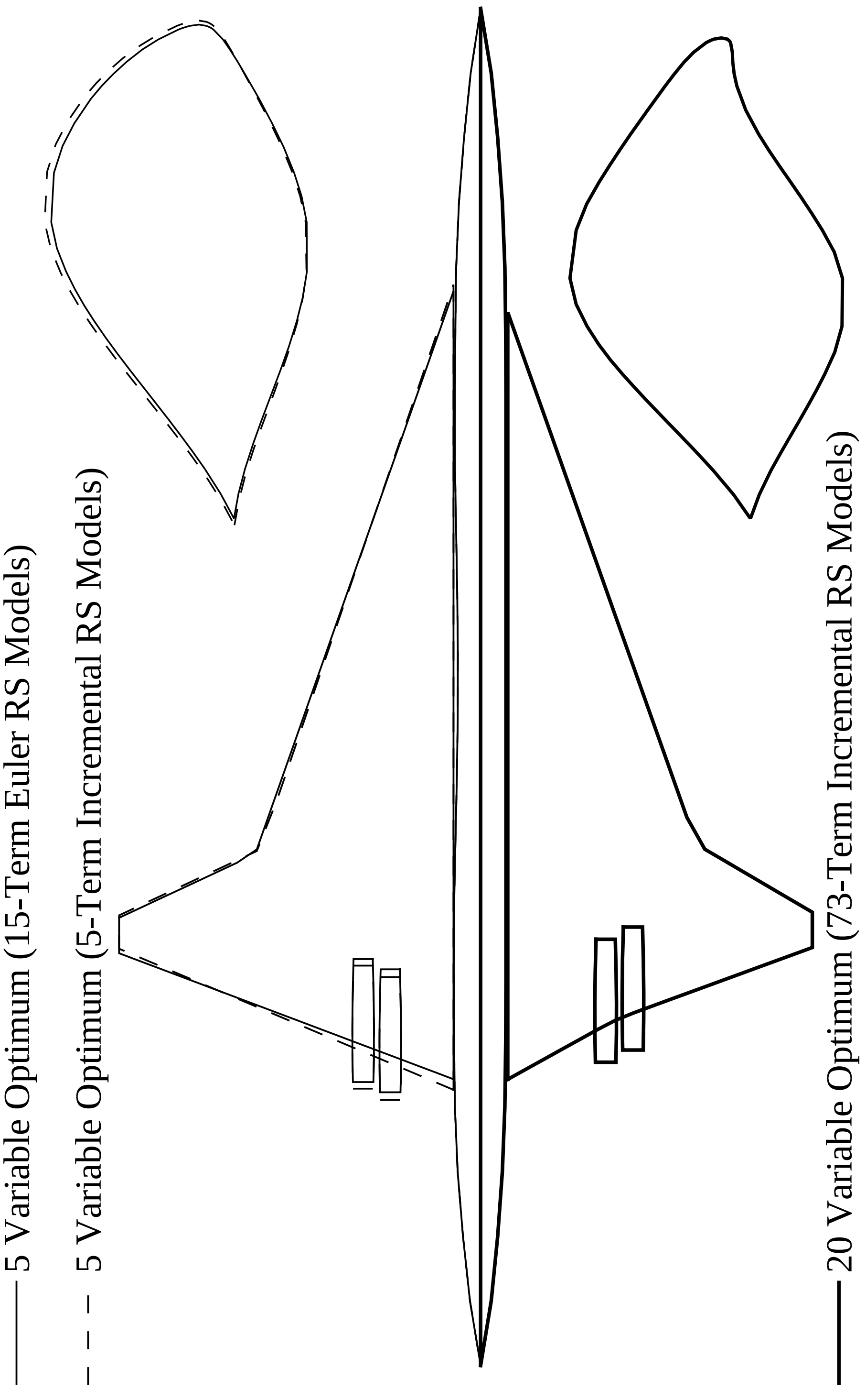

Figure 6: Optimal Configurations from the Five and Twenty Variable Design Problems.

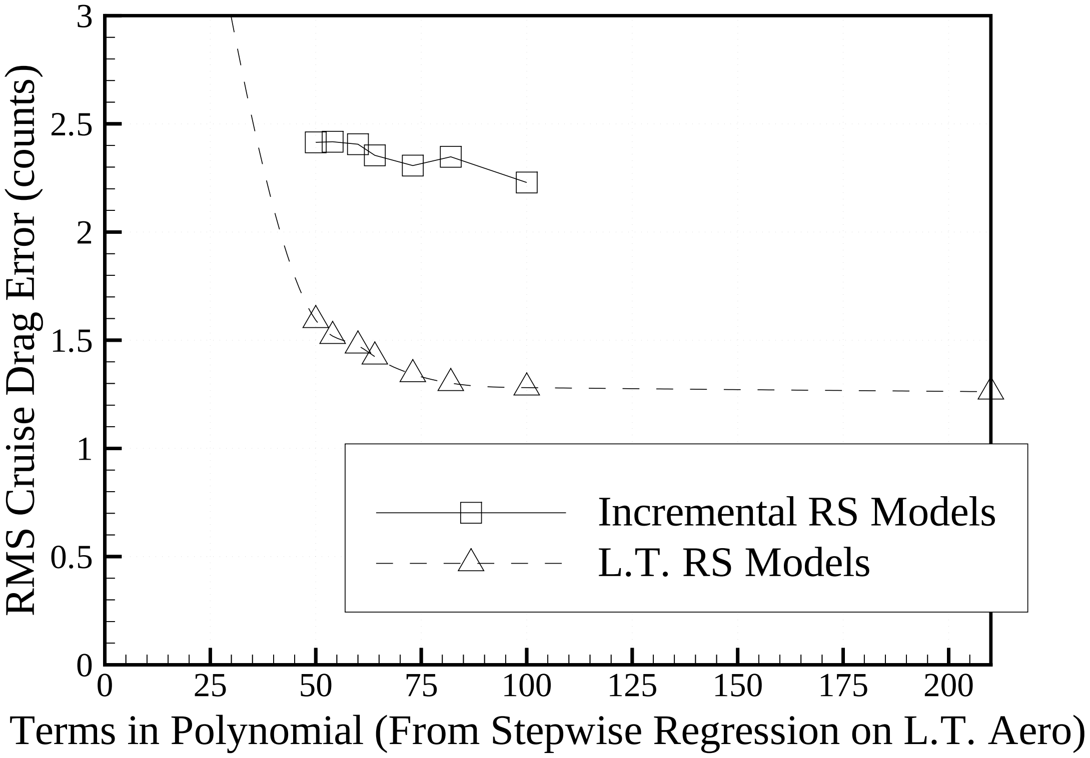

Figure 7: Stepwise Regression (20 Variable Problem).

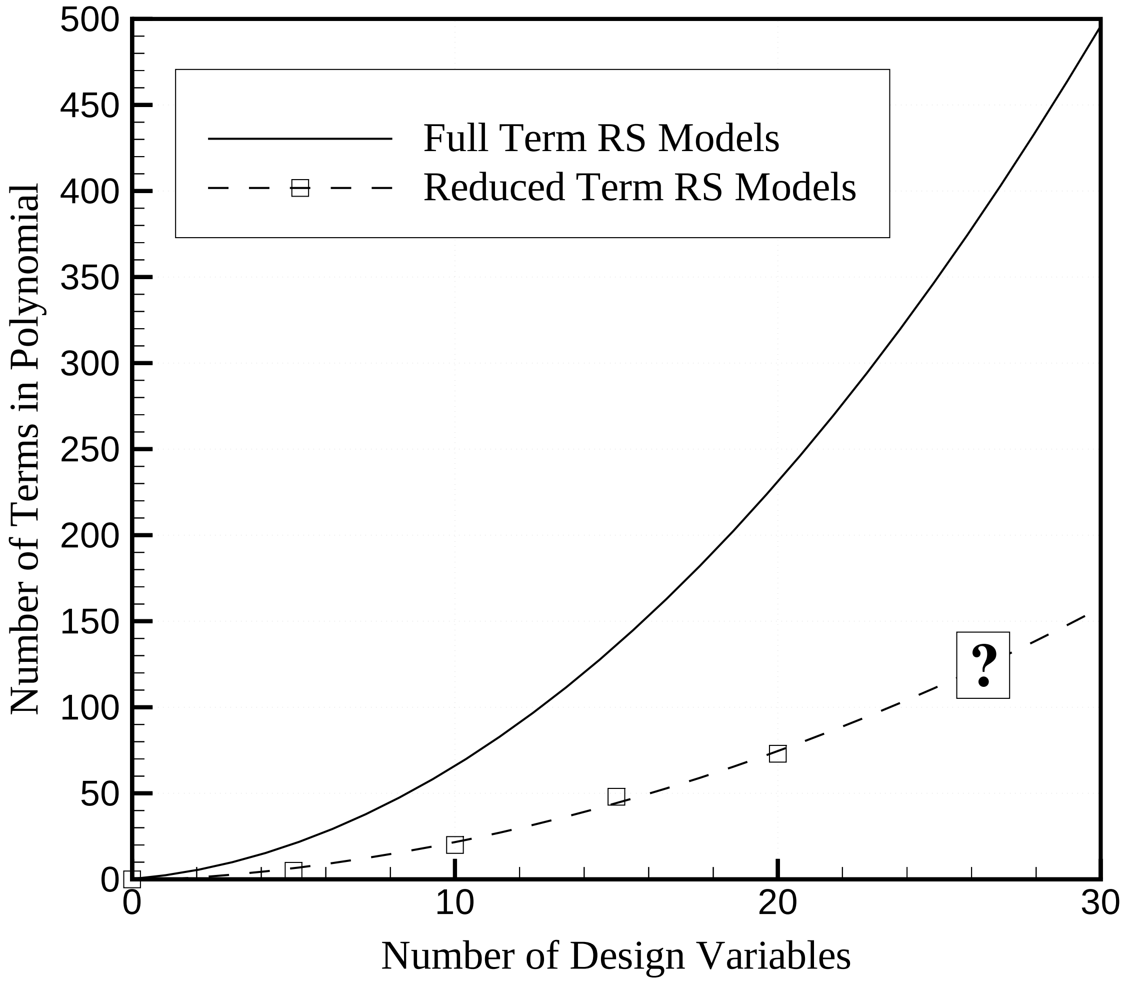

Figure 8: Number of terms in RS Models.